Published in final edited form as:
J Neurochem. 2009 March ; 108(6): 1561–1574. doi:10.1111/j.1471-4159.2009.05932.x.

Mutant Pink1 induces mitochondrial dysfunction in a neuronal cell model of Parkinson's disease by disturbing calcium flux

Roberta Marongiu[1,2], **Brian Spencer**[1], **Leslie Crews**[3], **Anthony Adame**[1], **Christina Patrick**[1], **Margarita Trejo**[1], **Bruno Dallapiccola**[2,4], **Enza Maria Valente**[2,5], and **Eliezer Masliah**[1,3]

[1]Dept. of Neurosciences, University of California, San Diego, La Jolla, CA 92093-0624 USA

[2]IRCCS CSS-Mendel Institute, Rome, ITALY

[3]Dept. of Pathology, University of California, San Diego, La Jolla, CA 92093-0624 USA

[4]Dept. of Experimental Medicine, Sapienza University, Rome, ITALY

[5]Dept. of Medical and Surgical Pediatric Sciences, University of Messina, Messina, ITALY

Abstract

Parkinson's disease (PD) is characterized by accumulation of α-synuclein and degeneration of neuronal populations in cortical and subcortical regions. Mitochondrial dysfunction has been considered a potential unifying factor in the pathogenesis of the disease. Mutations in genes linked to familial forms of PD, including *SNCA* encoding α-synuclein and *PINK1*, have been shown to disrupt mitochondrial activity. We investigated the mechanisms through which mutant Pink1 might disrupt mitochondrial function in neuronal cells with α-synuclein accumulation. For this purpose, a neuronal cell model of PD was infected with virally-delivered Pink1, and was analyzed for cell survival, mitochondrial activity and calcium flux. Mitochondrial morphology was analyzed by confocal and electron microscopy. These studies showed that mutant (W437X) but not wildtype Pink1 exacerbated the alterations in mitochondrial function promoted by mutant (A53T) α-synuclein. This effect was associated with increased intracellular calcium levels. Co-expression of both mutant Pink1 and α-synuclein led to alterations in mitochondrial structure and neurite outgrowth that were partially ameliorated by treatment with Cyclosporine A, and completely restored by treatment with the mitochondrial calcium influx blocker Ruthenium Red, but not with other cellular calcium flux blockers. Our data suggest a role for mitochondrial calcium influx in the mechanisms of mitochondrial and neuronal dysfunction in PD. Moreover, these studies support an important function for Pink1 in regulating mitochondrial activity under stress conditions.

Keywords

α-synuclein; Pink1; Parkinson's; mitochondria; calcium

Introduction

Parkinson's Disease (PD) is one of the most common neurodegenerative disorders in the elderly, with age-related prevalence reaching 2% in the seventh decade (Dauer *et al.* 2002, Dauer & Przedborski 2003). The classic form of PD is manifested clinically by resting tremor, rigidity, bradykinesia and postural instability, along with variable non-motor

Correspondence and reprint requests should be addressed to: Dr. E. Masliah, Department of Neurosciences, University of California San Diego, La Jolla, CA 92093-0624 Phone (858) 534-8992, Fax (858) 534-6232, emasliah@ucsd.edu.

symptoms. Neuropathologically, PD is characterized by the loss of dopaminergic neurons mainly in the substantia nigra pars compacta (Hirsch *et al.* 1999), accompanied by the formation of intracytoplasmic inclusions known as Lewy bodies. Moreover, neurodegeneration also occurs in other brain regions including the limbic system (Braak & Braak 2000). The primary component of these inclusions is fibrillar α-synuclein (α-syn), which is often highly ubiquitinated (Spillantini *et al.* 1997, Takeda *et al.* 1998, Wakabayashi *et al.* 1997, Hasegawa *et al.* 2002).

Missense mutations and multiplications of the *SNCA* gene encoding α-syn represent a rare cause of autosomal dominant parkinsonism (Tan & Skipper 2007). α-syn is a highly conserved presynaptic protein of about 14 kDa that under physiological conditions is likely involved in chaperone function (Souza *et al.* 2000), vesicular release of neurotransmitters (Leng *et al.* 2001, Liu *et al.* 2004), and tyrosine hydroxylase regulation (Yu *et al.* 2004), among other possibilities. Abnormal accumulation and oligomerization of α-syn has been proposed to play an important role in PD pathogenesis. Indeed, *in vitro* studies have shown that α-syn mutations and overexpression accelerate the oligomerization process (Conway *et al.* 1998, Narhi *et al.* 1999, Conway *et al.* 2000), and a similar increase in protein aggregation has been detected in the brain of α-syn transgenic mice, whose clinical features resemble those of PD (Chesselet 2008, Masliah *et al.* 2000, Lee *et al.* 2002, Giasson *et al.* 2002). Several lines of evidence suggest that mitochondrial dysfunction is among the main consequences of α-syn aggregation (Cookson & van der Brug 2008). Indeed, overexpression of wildtype (wt) and mutant α-syn in cellular and animal models has been shown to alter mitochondrial function by disrupting mitochondrial respiratory chain activity (Hsu *et al.* 2000, Elkon *et al.* 2002, Smith *et al.* 2005, Martin *et al.* 2006, Devi *et al.* 2008), raising intracellular and intramitochondrial Ca2+ levels (Adamczyk & Strosznajder 2006, Danzer *et al.* 2007, Parihar *et al.* 2008, Martinez *et al.* 2003) and increasing membrane ion permeability (Furukawa *et al.* 2006, Volles & Lansbury 2002, Martinez et al. 2003). Moreover, recent studies have demonstrated that α-syn can accumulate into mitochondria, residing mostly at the inner membrane (Parihar et al. 2008, Li *et al.* 2007, Devi et al. 2008).

In addition to *SNCA*, other genes have been identified that cause hereditary forms of PD (Tan & Skipper 2007). The functional characterization of their protein products has further confirmed the key role of mitochondria in PD pathogenesis (Abou-Sleiman *et al.* 2006), in line with previous results obtained in neurotoxic models (Langston *et al.* 1983, Betarbet *et al.* 2000, Heikkila *et al.* 1985) and in PD patients (Betarbet et al. 2000, Langston et al. 1983, Mizuno *et al.* 1989, Schapira *et al.* 1989, Thyagarajan *et al.* 2000). In particular, the identification of Pten-induced putative kinase 1 (*PINK1)* mutations in patients with autosomal recessive parkinsonism provided the first evidence of a direct link between dysfunction of a mitochondrial protein and PD (Valente *et al.* 2004).

Pink1 is a ubiquitously expressed 581-amino acid protein with an N-terminal mitochondrial targeting motif, a highly conserved serine/threonine kinase domain and a C-terminal autoregulatory region. Although its functions are only partially understood, Pink1 has been shown to protect neuronal cells from a number of cellular stresses by maintaining mitochondrial membrane potential and mitochondrial structure, and reducing cytochrome C release and activation of the apoptotic cascade (Deng *et al.* 2005, Petit *et al.* 2005, Pridgeon *et al.* 2007, Exner *et al.* 2007, Haque *et al.* 2008). Pink1 has been demonstrated to interact with other PD-related proteins. The most representative example is Parkin, an E3 ubiquitin-ligase that, when mutated, causes early-onset parkinsonism. Indeed, recent studies on drosophila and cellular models showed that Pink1 and Parkin could act in the same pathway implicated in the maintenance of mitochondrial integrity and function, with Parkin downstream of Pink1 (Pallanck & Greenamyre 2006, Exner et al. 2007).

Although this recent evidence supports a role for mitochondrial dysfunction in Pink1 mutation, less is known about the mechanisms involved. In this context, the main objective of this study was to investigate the mechanisms through which mutant Pink1 might disrupt mitochondrial function in a neuronal cell model of α-syn accumulation. We report that in this system, mut Pink1 promotes mitochondrial dysfunction and reduced neural plasticity by altering mitochondrial calcium flux.

Materials and methods

Materials

A polyclonal antibody for α-syn and a monoclonal antibody for the hemagglutinin (HA) tag (to detect Pink1) were purchased from Chemicon (Temecula, CA) and Roche (Palo Alto, CA) respectively. Lactase Dehydrogenase Activity Assay (LDH assay), 3-(4,5-Dimethylthiazol-2-yl)-2,5-diphenyltetrazolium bromide (MTT) and ATP assay kits were from Promega (San Luis Obispo, CA). Mitotracker MCXRos was purchased from Molecular Probes (Carlsbad, CA). Ruthenium Red (RR), Cobalt Chloride (CC), Flufenamic Acid (FFA), Cyclosporine A (CsA) were all purchased from Sigma (St. Louis, MO).

Generation of lentiviruses expressing α-syn and Pink1

cDNAs for *SNCA* and *PINK1* genes were first synthesized and cloned into expression vectors. Human wt and W437X *PINK1* cDNA was cloned into pcDNA3.1-HA vector (Invitrogen, Carlsbad, CA) as previously described (Silvestri *et al.* 2005). Human wt and A53T *SNCA* cDNA was cloned into pCEP4 vector (Invitrogen, Carlsbad, CA) as previously described (Hashimoto *et al.* 1997, Takenouchi *et al.* 2001)

cDNAs were then cloned into the third generation lentivirus (LV) vector pBOB with XbaI and BamHI sites. LVs expressing Pink1 (both wt and mutant W437X), α-syn (both wt and mutant A53T), green fluorescent protein (GFP) or empty vector (as controls) were prepared by transient transfection in 293T cells (Naldini & Verma 2000).

Establishment of a neuronal cell line expressing α-syn and Pink1

For these experiments we used the rat neuroblastoma cell line B103. This model was selected because overexpression of α-syn in these cells interferes with neuronal plasticity (reduced neurite outgrowth and adhesion) but does not result in overt cell death(Takenouchi et al. 2001, Hashimoto *et al.* 2003). Furthermore, these cells display mitochondrial alterations and abnormal accumulation of oligomeric α-syn (Takenouchi et al. 2001, Hashimoto et al. 2003). This model mimics the early pathogenic process of PD where dopaminergic cell death is preceded by reduced neurite outgrowth and synaptic alterations (Takenouchi et al. 2001, Hashimoto et al. 2003). For all experiments, cells were plated in complete media and infected with LVs expressing wt or mutant Pink1 and wt or mutant α-syn at a multiplicity of infection (MOI) of 40. After infection, cells were incubated for 48 h in a humidified 5% CO2 atmosphere at 37°C. All experiments were conducted in triplicate to ensure reproducibility.

Immunoblot analysis

Cells were lysed in TNE buffer (50 mM Tris-HCl, pH 7.4, 150 mM NaCl, 1 mM EDTA; all from Sigma-Aldrich) containing 1% Nonidet P-40 (Calbiochem) with protease and phosphatase inhibitor cocktails (Roche). Total cell extracts were centrifuged at 6,000 × g for 15 min, and the protein concentration of supernatants was assayed with a BCA protein assay kit (Pierce Biotechnology, Rockford, IL). For Western blot analysis, 20 μg of lysate per lane were loaded into 4–12% Bis-Tris SDS-PAGE gels and blotted onto polyvinylidene fluoride

(PVDF) membranes. Blots were incubated with antibodies against α-syn and against HA, followed by secondary antibodies tagged with horseradish peroxidase (1:5000, Santa Cruz Biotechnology, Inc.), visualized by enhanced chemiluminescence and analyzed with a Versadoc XL imaging apparatus (BioRad, Hercules, CA). Analysis of actin levels was used as a loading control.

Immunofluorescent confocal microscopy

To verify expression levels of α-syn or Pink1 in cells infected with the different LV vectors, cells were seeded onto poly L-lysine-coated glass coverslips, grown to 60% confluence and fixed in 4% paraformaldehyde (PFA) for 20 minutes. Coverslips were pre-treated with 0.1% Triton X-100 in TBS for 20 min and then incubated overnight at 4°C either with the antibody against human α-syn (1:500) or anti-HA (1:250). The following day, antibodies were detected with the fluorescein isothiocyanate (FITC)-conjugated secondary antibody (Vector Laboratories, Burlingame, CA, USA). Control samples included: empty vector or GFP-infected cells, and immunolabeling in the absence of primary antibodies. Coverslips were mounted with Prolong Gold anti-fading reagent with DAPI (Invitrogen). Cells were analyzed with a digital epi-flourescent microscope (Olympus BX51) to estimate percentage of total cells (DAPI stained) that displayed GFP, α-syn or HA (Pink1) reactivity.

To verify the co-expression of α-syn and Pink1 in cells co-infected with different LV vectors, coverslips were double-labeled as previously described (Crews *et al.* 2008). Coverslips were air-dried, mounted on slides with anti-fading media (Vectashield, Vector Laboratories), and imaged with confocal microscope MRC1024 (BioRad). An average of 50 cells per condition were imaged and the individual channel images were merged and analyzed with the Image J program.

Analysis of LC3 levels

To investigate if the enlarged electrodense bodies in neuronal cells expressing mutant Pink1 and α-syn corresponded to an autophagy response, LC3 levels were analyzed in coverslips with LC3-GFP and by immunoblot. B103 cells were grown as described above and were then plated onto poly L-lysine coated glass coverslips at a density of 5×10^4 cells. Five hours after plating, cells were infected with the LV-α-syn and/or LV-Pink 1 and incubated for 48 hours. All coverslips were also co-infected with a lentiviral vector expressing LC3-GFP at an MOI of 40. Cultures were then washed 2X with serum-free DMEM and then fed either complete media or serum-free media for 12 hours before fixation with 4% PFA. Briefly as previously described (Pickford *et al.* 2008), coverslips were treated with Prolong Gold antifading reagent with DAPI (Invitrogen) and imaged with the LSCM to determine the number of GFP-positive granular structures consistent with autophagolysosomes using semiautomatic image analysis system and the ImageQuant software. For each condition an average of 50 cells were analyzed. In addition, LC3 levels were analyzed by western blot. Briefly, as previously described (Pickford et al. 2008), cells were infected with LV-α-syn and/or LV-Pink 1 for 72 hours then lysed in TNE buffer (50 mM Tris-HCl, pH 7.4, 150 mM NaCl, 1 mM EDTA; all from Sigma-Aldrich) containing 1% Nonidet P-40 (Calbiochem) with protease and phosphatase inhibitor cocktails (Roche). 20 μg of lysate per lane were loaded into 4–12% Bis-Tris SDS-PAGE gels and blotted onto polyvinylidene fluoride (PVDF) membranes. Blots were incubated with the rabbit polyclonal antibody against LC3 (recognizes LC3-I and LC3-II, Abcam), followed by secondary antibodies tagged with horseradish peroxidase (1:5000, Santa Cruz Biotechnology, Inc.), visualized by enhanced chemiluminescence and analyzed with a Versadoc XL imaging apparatus (BioRad, Hercules, CA). Analysis of actin levels was used as a loading control.

Evaluation of mitochondrial morphology and membrane potential by Mitotracker

Mitochondrial morphology and damage to mitochondrial membrane integrity were examined using the membrane permeable dye Mitotracker Red MCXRos (Invitrogen). This dye is rapidly taken up into negatively charged mitochondria, allowing to assess alterations in mitochondrial morphology and to qualitatively estimate variations in the mitochondrial membrane potential ($\Delta\Psi_m$) (Buckman *et al.* 2001). Cells were plated on poly-L-Lysine coated coverslips, grown to 60% confluence and infected with LVs as described above. Mitotracker staining was performed according to the manufacturer's protocol and coverslips imaged with the laser scanning confocal microscope. Experiments were also conducted in presence of either CsA or the cellular calcium inhibitors RR (10μM), CC (5μM), and FFA (40μM). Briefly as previously described (Langford *et al.* 2004), an average of 200 cells per condition were obtained and average pixel intensity levels were determined using ImageQuant software (Molecular Dynamics, Piscataway, NJ). The digitized images obtained for each of these conditions were also analyzed with the NIH Image J program to determine the average mitochondrial diameter.

To determine the co-localization between α-syn or Pink1 with the mitochondria, coverslips stained with the Mitotracker were fixed in 4% PFA for 20 minutes and immunostained with the antibodies against α-syn or HA. The primary antibodies were detected with the FITC-conjugated secondary antibody (Vector Laboratories, Burlingame, CA, USA) and examined with the laser scanning confocal microscope. An average of 50 cells per condition were imaged and the individual channel images were merged and analyzed with the Image J program.

Electron microscopy

Briefly, B103 neuronal cells were plated in 35 mm dishes with a coverslip in the bottom and infected with LVs. After 48 h, cells were fixed in 2% paraformaldehyde and 1% glutaraldehyde, then fixed in osmium tetroxide and embedded in epon araldite. Once the resin hardened, blocks with the cells were detached from the coverslips and mounted for sectioning with an ultramicrotome (Leica). Further characterization of the presence of Pink1 in the mitochondria was performed by immunoelectron microscopic analysis. Briefly as previously described (Masliah *et al.* 2001), cells on coverslips were embedded in epoxy araldite, followed by ultra-thin sectioning. Sections were placed on formvar-coated grids, etched and then immunolabeled with an antibody against HA (for detection of HA-tagged Pink1) or an antibody against α-syn, followed by labeling with 10 nm Aurion ImmunoGold particles (1:50, Electron Microscopy Sciences, Fort Washington, PA) with silver enhancement. Grids were analyzed with a Zeiss OM 10 electron microscope as previously described (Rockenstein *et al.* 2001).

MTT, LDH, TUNEL and neurite length assays

Mitochondrial activity, cell death and apoptosis were evaluated via the MTT, LDH and TUNEL assays as previously described (Langford et al. 2004). Cells were plated on 96 well plates in complete media. For treatments, cells were transferred to minimal media (1% serum) and assays were then performed following manufacturer's instructions (Promega). To evaluate neurite outgrowth and adhesion, an average of 100 neurons per condition were imaged with phase contrast microscopy and neurite length estimated with the ImageQuant software.

Measurement of cellular ATP production

Cellular ATP levels were measured using the ATP luminescent assay kit, Cell Titer-Glo (Promega). Cells were seeded onto black clear-bottom 96 well plates in complete media,

infected and incubated for 48h. After treatment, ATP assay was performed according to the manufacturer's instructions. Briefly, 100 μl of reaction solution was added to each well and incubated for 2 min at RT, followed by detection of luminescence in a plate reader (Beckman Coulter, DTX880). ATP assay was also performed after treating infected cells with various pharmacological agents. Experiments were conducted either in presence of the cyclophilin D inhibitor CsA (5μM) or various cellular calcium inhibitors including RR (10μM), CC (5μM), and FFA (40μM).

Calcium mobilization assay

Assessment of calcium influx was carried out using a modified protocol of the FLIPR 4 calcium assay (Molecular Devices, Sunnyvale, CA). Briefly, B013 cells were infected with LV constructs at a MOI of 30 and were cultured in DMEM medium (Mediatech, Manassas, VA) containing 10% FBS and penicillin/streptomycin. Cultures were maintained in an incubator at 37° C, in an atmosphere of 95% air and 5% CO_2. Two days after infection, cells were plated at a density of 30,000 cells/well on Costar 96 well-black plates with flat clear bottom (Corning, Corning, NY). Following inhibitor treatments, media was replaced by 100 μl of HBSS buffer and 100 μl of calcium dye was added to each well. Cells were kept in the incubator at 37°C for 1 hr before measuring fluorescence with excitation/emission filter at 470–495/515–575 nm on a DTX 880 Multimode Detector (Beckman Coulter, Fullerton, CA). As a positive control of calcium influx, 0.6 μg of ionomycin (Sigma, St. Louis, MO) was added to one set of wells.

Statistical analysis

All experiments were performed blind coded and in triplicate. Values in the figures are expressed as means ± SEM. To determine the statistical significance, values were compared by using the one-way ANOVA with post-hoc Dunnett's test when comparing the LV-α-syn A53T and/or Pink1 W437X to LV-control. Additional comparisons were done using Tukey-Kramer post-hoc test when comparing the combined LV-α-syn A53T and Pink1 W437X to cells singly-infected with LV expressing the mutant genes. The differences were considered to be significant if p values were less than 0.05.

Results

Characterization of Pink1 and α-syn expression in neuronal cell lines infected with lentiviral vectors

To investigate the effects of Pink1 in a neuronal cell model of α-syn accumulation, SNCA and PINK1 cDNAs were cloned into lentiviral vectors and viruses were used to infect B103 neuronal cells. This cell line was derived from rat neuroblastoma and shares many typical neuronal properties with other commonly used neuronal cell lines, including outgrowth of neurites, synthesis of neurotransmitters, possession of neurotransmitter receptors, and electrical excitability of surface membranes (Schubert *et al.* 1974). Compared to cells infected with empty vector LV-control (Fig. 1A), infection of the B103 cells with LV-GFP at a MOI of 40 resulted in GFP expression in about 90% of plated cells (Fig. 1B). Immunocytochemical analysis with antibodies against α-syn and HA (to detect Pink1), showed high levels of expression in over 85% of the cells singly infected with the LVs containing wt or mutant α-syn (Fig. 1C,D) and wt or mutant Pink1 (Fig. 1E,F). Confocal imaging in cells co-infected with LV-α-syn (wt or A53T) and LV-Pink1 (wt or W437X) showed that about 70–80% of cells expressed both proteins (Supplemental Fig. 1). By immunoblot, α-syn was detected at comparable levels in B103 neuronal cells infected with LV-α-syn wt and A53T (Fig. 1G). For cells infected with the LV-Pink1 wt this protein was detected as a strong band at 65 kDa and a weaker band at 45 KDa, while W437X Pink1 was identified as two bands at 47 and 35 kDa (Fig. 1G).

Mutant Pink1 promotes structural mitochondrial alterations in α-syn-expressing neuronal cells

We next compared the characteristics of mitochondria in α-syn-expressing neuronal cells co-infected with wt or mut Pink1 using Mitotracker Red. In cells infected with empty LV vector, LV-GFP, LV-α-syn wt or LV-Pink1 wt, mitochondria appeared as discrete punctate or elongated structures (Fig. 2A-C) with a mean diameter of 0.76 μm (Fig. 2G), occupying on average 8% of the cell surface area (data not shown). Since both empty LV vector (referred to as LV-control) and LV-GFP gave comparable results, subsequent experiments were performed with the LV-control to avoid interference in the fluorescent channel for the image analysis and double labeling experiments.

Neuronal cells expressing the LV-α-syn A53T (Fig. 2D) or Pink1 W437X (Fig. 2E) showed significant alterations in mitochondrial morphology including irregular profiles and increased size (Fig. 2G). These alterations were exacerbated in cells co-infected with mutant forms of both α-syn and Pink1 (LV-α-syn A53T and LV-Pink1 W437X) (Fig. 2F,G). However cells expressing a mutant form of only α-syn or Pink1 (α-syn A53T and Pink1 wt or α-syn wt and Pink1 W427X) were not significantly different from their singly-infected counterparts (Fig. 2G).

To further investigate the characteristics of mitochondrial alterations in neuronal cells overexpressing α-syn and Pink1, ultrastructural analysis was performed. Consistent with the confocal microscopy data (Fig. 2), compared to LV-control (Fig. 3A,B), neuronal cells infected with LV-α-syn A53T (Fig. 3C,D) or LV-Pink1 W437X (Fig. 3E,F) displayed significant subcellular alterations including enlarged and irregular mitochondria. In cells co-expressing both mutant proteins (Fig. 3G,H and Fig. 4) these alterations were more severe, with mitochondria that were often enlarged (Fig. 4B) or elongated (Fig. 4C), with abnormal cristae and accumulation of occasional single electrodense inclusions (Fig. 4D). Moreover, abnormally enlarged autophagolysosomes containing abundant electrodense inclusions were often encountered in close proximity to the enlarged mitochondria (Fig. 4B and supplemental Fig. 2), and these were also often surrounded by filamentous aggregates ranging in diameter between 9–11 nm (Fig. 4E,F).

To validate the ultrastructural data and to determine whether the enlarged electrodense bodies in neuronal cells expressing mutant Pink1 and α-syn corresponded to an autophagy response potentially associated with the turnover of dysfunctional mitochondria, LC3 expression patterns were analyzed by confocal microscopy in B103 cells expressing GFP-tagged LC3. These studies showed that compared to LC3-GFP-expressing cells infected with vector control (Supplemental Fig. 3A,G), cells co-expressing LC3-GFP and LV-α-syn wt, LV-α-syn A53T, or LV-Pink1 W437X displayed increased GFP fluorescence corresponding to increased levels of LC3 expression (Supplemental Fig. 3B-D,G). This effect was enhanced in cells co-infected with LV-Pink1 W437X, where LC3-GFP accumulated in discrete cytoplasmic aggregates (Supplemental Fig. 3D-F,G). Consistent with the confocal microscopy results, immunoblot analysis of LC3 immunoreactivity in B103 cells showed that compared to cells infected with LV-control, cells infected LV-α-syn displayed increased levels of LC3 (Supplemental Fig. 3H,I).

To further investigate a role of Pink1 in mediating mitochondrial damage in a cellular model of PD that expresses α-syn at high levels, co-localization studies were performed. Neuronal cells expressing Pink1 wt (Fig. 5A-C) or α-syn wt (Fig. 5D-F) displayed a more diffuse immunoreactivity that was less often co-localized around mitochondria. In contrast, in neuronal cells infected with LV-Pink1 W437X (Fig. 5G-I), the immunoreactivity for Pink1 was in closer proximity to mitochondria stained with Mitotracker. Similarly, in neuronal cells infected with LV-α-syn A53T (Fig. 5J-L), α-syn immunoreactivity was detected

around the mitochondria (Fig. 5G-L). This effect—demonstrated in more detail in Fig. 5M-O—became more evident in cells co-infected with LV-α-syn A53T and LV-Pink1 W437X (Fig. 5P-R).

Electron microscopic analysis of B103 neuronal cells expressing Pink1 and immunolabeled with an antibody against HA confirmed the presence of abundant gold particles in the mitochondria of mut Pink1-infected cells and to a lesser extent in the wt Pink1 compared to controls (Supplemental Fig. 4). The gold particles tended to be associated with the inner mitochondrial membrane. In control experiments where the primary antibody was excluded or in uninfected neuronal cells, only scattered gold particles were observed in the cytoplasm, but there was no association with mitochondria.

Mutant Pink1-associated mitochondrial structural alterations result in mitochondrial functional deficits in α-syn-expressing neuronal cells

To determine if mut Pink1-mediated mitochondrial structural alterations were associated with functional deficits, the mitochondrial $\Delta\Psi_m$ was estimated semi-quantitatively by analyzing Mitotracker Red fluorescence (Fig. 6). Compared to cells infected with LV-control or wt α-syn or Pink1, cells expressing either α-syn A53T or Pink1 W437X displayed a mild but significant 18–20% reduction in $\Delta\Psi_m$ ($p<0.05$). Co-expression of both mutant proteins resulted in a marked deficit of $\Delta\Psi_m$ (45%, $p<0.05$) (Fig. 6A).

Further assessment of mitochondrial activity was performed by analyzing levels of ATP production. Neuronal cells expressing α-syn wt or A53T, either alone or associated with Pink1 wt did not show any significant ATP reduction compared to controls (Fig. 6D). Conversely, the presence of mutant Pink1 severely affected ATP production, which was progressively reduced in cells expressing Pink1 W437X alone (~16%, $p<0.05$) or in combination with α-syn wt (~21%, $p<0.05$) (Fig. 6D). Consistent with the structural and membrane potential studies, cells expressing Pink1 W437X associated with mutant α-syn showed the most severe reduction in ATP levels (~40%, $p<0.05$) (Fig. 6D).

Furthermore, the MTT assay showed significantly reduced values (~20%, $p<0.05$) in cells expressing mutant α-syn, either alone or in combination with Pink1 wt or W437X (Fig. 7A), suggesting that this assay is more sensitive to α-syn- than Pink1-induced alterations. These deficits in neuronal function were not related to compromised cell viability because neither LDH nor TUNEL assays showed significantly increased levels of cell death during 48 h in the presence of mutant α-syn and/or Pink1 (Supplemental Fig. 5). We have previously shown that in stably transfected B103 neuronal cells, α-syn overexpression results in decreased adhesion and neurite outgrowth (Takenouchi et al. 2001). In agreement with this, cells infected with LV-α-syn A53T or Pink1 W437X displayed a moderate but significant reduction in neurite length (~30%, $p<0.05$) (Fig. 7D). This decrease dramatically worsened in cells co-infected with both mutant α-syn and Pink1 (~60%, $p<0.05$), while it was ameliorated when one mutant protein was co-expressed with the other wt protein (Fig. 7D).

Mitochondrial alterations associated with mutant Pink1 are partially reversed by Cyclosporine A in α-syn-expressing neuronal cells

Reduced ATP production and loss of $\Delta\Psi_m$ can promote the opening of mitochondrial permeability transition pore (mPTP) (Crompton 1999), which in turn could lead to neuronal dysfunction. To evaluate if alterations in the mPTP opening play a role in mitochondrial dysfunction in the α-syn-expressing neuronal cells infected with LV-Pink1 mut, cells were treated with Cyclosporine A (CsA), a pharmacological agent known to inhibit cyclophilin D, one of the components of the mPTP (Waldmeier *et al.* 2003). Treatment with CsA was able to recover the $\Delta\Psi_m$ in neuronal cells co-expressing α-syn A53T and Pink1 W437X (Fig.

6B). Similarly, CsA restored ATP levels (Fig. 6E), MTT activity (Fig. 7B) and neurite outgrowth (Fig. 7E) back to the baseline in neuronal cells expressing Pink1 W437X alone or in combination with α-syn wt, while it partially rescued the severe reduction of ATP levels (Fig. 6E) and neurite length (Fig. 7E) in cells expressing both mutant proteins (from a 40% under basal media to a 20% loss with CsA). These results suggest that alterations in mPTP might play a role in the deleterious effects of mutant α-syn and Pink1.

Blockage of mitochondrial calcium influx completely rescues mitochondria from damage induced by mutant Pink1 in α-syn-expressing neuronal cells

An excessive electrogenic entry of free calcium into mitochondria through its specific channel is one of the best-known causes of ATP synthesis disruption, likely by direct inhibition of the respiratory chain function and alteration of $\Delta\Psi_m$ (Mattson 2007, Parihar et al. 2008). To determine whether the mitochondrial membrane damage and ATP reduction observed in α-syn-expressing cells infected with LV-Pink1 mut might be due to a mitochondrial calcium overload, cells were separately treated with different calcium channels blockers. These included Cobalt Chloride (CC), which prevents extracellular calcium influx, Flufenamic Acid (FFA), which blocks endoplasmic reticulum calcium flux, and Ruthenium Red (RR), a specific mitochondrial calcium uptake channel blocker.

Only RR treatment was able to restore $\Delta\Psi_m$ to normal levels in cells infected with LV α-syn A53T and Pink1 W437X (Fig. 6C and supplemental Fig. 6). Compared to LV-control, neither CC nor FFA were able to restore mitochondrial membrane damage associated with the expression of LV α-syn A53T and Pink1 W437X (~20–40% loss, $p<0.05$) (Fig. 8A-C and supplemental Fig. 6). Similarly, treatment with RR completely re-established ATP levels (Fig. 6F), MTT activity (Fig. 7C) and neurite outgrowth (Fig. 7F) to normal values in cells that expressed Pink1 W437X, alone or in combination with α-syn wt and A53T. In contrast, neither CC nor FFA was able to restore the ATP loss (~15–40%, $p<0.05$) in neuronal cells infected with LV α-syn A53T and Pink1 W437X (Fig. 8D-F).

Mutant Pink1-related mitochondrial functional deficits in α-syn-expressing neuronal cells are associated with increased calcium flux

To further investigate the possibility that the mitochondrial alterations in α-syn-expressing neuronal cells infected with LV-Pink1 mut might be associated with aberrant calcium flux, levels of intracellular calcium were determined with the fluorescent calcium indicator Fluo-4. Compared to B103 cells infected with a LV-control, cells infected with LV-α-syn wt or A53T displayed a 25–50% ($p<0.05$) increase in intracellular calcium (Fig. 9A). Expression of Pink1 wt alone or in combination with α-syn showed calcium levels similar to controls, however cells expressing Pink1 mut showed increased calcium flux that was exacerbated in cells expressing both α-syn mut and Pink1 mut (Fig. 9A). Consistent with effects of calcium channel blockers in the Mitotracker, ATP, MTT and neurite outgrowth assays, RR prevented the increased calcium flux in α-syn and Pink1 mut expressing cells (Fig. 9B), while CC and FFA-treated cells (Fig. 9C,D) were similar to vehicle-treated controls (Fig. 9A). Taken together, these results support the possibility that mitochondrial alterations in α-syn-expressing neuronal cells infected with LV-Pink1 mut might be related to increased intracellular calcium that results in mitochondrial calcium overload.

Discussion

Growing evidence indicates that both α-syn and Pink1, two proteins mutated in familial PD, may disrupt mitochondrial structure and function leading to neurodegeneration. The present work investigated the mechanisms through which mutant Pink1 might disrupt mitochondrial function in a neuronal cell model of α-syn accumulation. We found that mutant Pink1

exacerbated the mitochondrial pathology associated with accumulation of α-syn by dysregulating mitochondrial calcium flux. Alterations consistent with mitochondrial dysfunction in the mut α-syn model included reduced MTT activity, loss of $\Delta\Psi_m$ and increased mitochondrial size with loss of cristae and accumulation of electrodense and fibrillar material. These alterations, in conjunction with reduced ATP levels, were more apparent in α-syn-expressing cells infected with LV-Pink1 mut.

Ultrastructural analysis showed accumulation of electrodense and fibrillar material around the mitochondria, accompanied by extensive mitochondrial alterations including increased size, reduced cristae and irregular membrane profiles in α-syn-expressing cells infected with LV-Pink1 mut. In support of a role for Pink1 mut in mitochondrial morphological alterations, recent studies elucidating the role of Pink1 in mitochondrial dynamics show that inhibition of Pink1 leads to excessive fusion (Yang *et al.* 2008). This is consistent with our data showing enlarged mitochondria in loss-of-function Pink1 mut-expressing cells. Moreover, activation of mitochondrial fission machinery via overexpression of Drp1 suppresses the phenotype of mutant Pink1, suggesting that these functions could be therapeutic targets for protecting against the effects of Pink1 mutation (Deng *et al.* 2008).

In addition to the morphological alterations observed in mitochondria in α-syn-expressing cells infected with LV-Pink1 mut, several degenerated mitochondria also appeared in autophagolysosomes, which target the lysosomal degradation pathway. In support of this observation, it has already been demonstrated that mitochondrial membrane depolarization and ATP depletion leads to impaired mitochondrial trafficking (Zanelli *et al.* 2006, Chang & Reynolds 2006, Rintoul *et al.* 2006) and eventually to selective autophagic degradation of mitochondria—a process known as mitophagy (Nakada *et al.* 2001, Ono *et al.* 2001, Priault *et al.* 2005). The autophagic/lysosomal degradation pathway is one of the main cellular systems that is activated to prevent accumulation of misfolded and aggregated proteins and to remove damaged cellular structures, such as mitochondria (Dunn 1994, Ravikumar *et al.* 2002, Webb *et al.* 2003). Indeed, autophagy has been increasingly recognized to play an important role in the maintenance of neuronal homeostasis, and alterations in its machinery has been related to the pathogenesis of major neurodegenerative disorders such as PD and Alzheimer's disease (Rubinsztein 2006, Ventruti & Cuervo 2007). The same α-syn is known to be degraded via the autophagy pathway and, when mutated, can lead to impairment of the autophagy machinery (Cuervo *et al.* 2004, Pan *et al.* 2008). There are three types of autophagy, including macroautophagy, microautophagy and chaperone-mediated autophagy (Seglen & Bohley 1992, Cuervo 2004). In macroautophagy, organelles and aggregated proteins are targeted for lysosomal degradation via an invagination of the cytoplasm known as an autophagic vacuole, or autophagosome (Cuervo 2004). Subsequent fusion with a lysosome, which introduces acid hydrolases into the vacuole, results in the generation of a single-membrane-bound degradative structure (the autophagolysosome) (Cuervo *et al.* 2005). Intriguingly, in this work we observed the presence of high numbers of enlarged autophagolysosomes surrounding dysfunctional mitochondria, and degenerated mitochondria in the autophagolysosomes. This might be due either to the activation of autophagy as a neuronal mechanism of defense from damage induced by co-expression of mutant α-syn and Pink1, or to the inhibition of this clearance system caused by the accumulation of both mutant proteins. Further studies will be necessary to clarify this evidence.

The effect of mutant Pink1 on mitochondrial dysfunction in α-syn-expressing cells supports a possible dominant negative mechanism of W437X Pink1 (Bonifati *et al.* 2005, Hatano *et al.* 2004, Hedrich *et al.* 2006, Pridgeon et al. 2007), and suggests that mutant Pink1 can reinforce α-syn pathology by acting independently on converging pathways affecting mitochondrial function. Additionally, although co-expression of α-syn A53T and Pink1

W437X did not lead to apoptotic cell death, it is possible that mitochondrial alterations and reduced ATP production might compromise neuronal function by reducing plasticity. In support of this possibility, we observed reduced neurite outgrowth in α-syn-expressing cells infected with LV-Pink1 mut.

Our data indicate mitochondrial calcium overload as responsible for the mitochondrial ATP and membrane potential reduction in mutant α-syn and Pink1 induced toxicity. Supporting this possibility, we showed that the mitochondrial calcium uptake channel blocker Ruthenium Red completely restored to baseline levels the mitochondrial ATP levels and membrane potential in neurons expressing mutant α-syn and/or Pink1. Conversely, blocking calcium influx in the cytoplasm with different compounds was unable to restore normal mitochondria activity.

Excess of intra-mitochondrial calcium has been shown to be responsible for the collapse of mitochondrial $\Delta\Psi_m$ (Cortassa *et al.* 2003), loss of respiratory control and impaired ATP synthesis (McCormack *et al.* 1990), and permeabilization of the mitochondrial inner membrane (Green & Reed 1998, Nicholls & Crompton 1980, Crompton 1999, Panov *et al.* 2002, Nicholls & Budd 2000). Moreover, an increased mitochondrial calcium load leads to opening of the mPTP, with cytochrome C release in the cytoplasm and activation of the apoptotic pathway (Brustovetsky *et al.* 2003). In support of a possible role of calcium-mediated opening of the mPTP in our system, we showed that CsA, a compound known to inhibit opening of mPTP, partially restored the mitochondrial alterations associated with co-expression of mutant α-syn and Pink1. Recent studies have shown that aggregated α-syn can be found within mitochondria (Lee *et al.* 2001), and this accumulation was directly related to an increase of intra-mitochondrial calcium levels, which in turn led to a raise of nitric oxide levels, oxidative damage and cytochrome C release (Li et al. 2007, Devi et al. 2008, Parihar et al. 2008). However, the actual mechanisms through which α-syn and Pink1 might promote excessive calcium accumulation in the mitochondria are not clear and require further assessment.

Alterations in mitochondrial function, increased calcium levels and dysfunctional autophagy have been shown to play a central role in the pathogenesis of a wide range of neurodegenerative disorders, including PD, Alzheimer's disease, Huntington's disease, and amyotrophic lateral sclerosis (ALS) (Orth & Schapira 2001, Ventruti & Cuervo 2007, Pan et al. 2008). Understanding the link between disease-related proteins, such as α-syn and Pink1, and mitochondrial homeostasis may represent a crucial step towards the development of mitochondrial-based therapeutic and neuroprotective strategies in PD and other neurodegenerative disorders.

Supplementary Material

Refer to Web version on PubMed Central for supplementary material.

Acknowledgments

This work was supported by grants from NIH (AG18440, AG10435 and AG022074), from Telethon Foundation Italy (GGP07210), from the Italian Ministry of Health (Progetto Ordinario Ricerca Finalizzata 2006; Ricerca Finalizzata 2006 ex. art 56). The support of Fondazione Livio Patrizi and Transgenomics is also gratefully acknowledged.

Abbreviations used in the text

α-syn	α-synuclein

CC	Cobalt Chloride
CsA	Cyclosporine A
FITC	fluorescein isothiocyanate
FFA	Flufenamic Acid
GFP	green fluorescent protein
HA	hemagglutinin
Pink1	Pten-induced putative kinase 1
LDH	Lactase Dehydrogenase
LV	lentivirus
MOI	multiplicity of infection
mPTP	mitochondrial permeability transition pore
MTT	3-(4,5-Dimethylthiazol-2-yl)-2,5-diphenyltetrazolium bromide
PD	Parkinson's disease
PFA	paraformaldehyde
PVDF	polyvinylidene fluoride
RR	Ruthenium Red
wt	wildtype

References

Abou-Sleiman PM, Muqit MM, Wood NW. Expanding insights of mitochondrial dysfunction in Parkinson's disease. Nat Rev Neurosci. 2006; 7:207–219. [PubMed: 16495942]

Adamczyk A, Strosznajder JB. Alpha-synuclein potentiates Ca2+ influx through voltage-dependent Ca2+ channels. Neuroreport. 2006; 17:1883–1886. [PubMed: 17179863]

Betarbet R, Sherer TB, MacKenzie G, Garcia-Osuna M, Panov AV, Greenamyre JT. Chronic systemic pesticide exposure reproduces features of Parkinson's disease. Nat Neurosci. 2000; 3:1301–1306. [PubMed: 11100151]

Bonifati V, Rohe CF, Breedveld GJ, et al. Early-onset parkinsonism associated with PINK1 mutations: frequency, genotypes, and phenotypes. Neurology. 2005; 65:87–95. [PubMed: 16009891]

Braak H, Braak E. Pathoanatomy of Parkinson's disease. J Neurol. 2000; 247(Suppl 2):II3–10. [PubMed: 10991663]

Brustovetsky N, Brustovetsky T, Purl KJ, Capano M, Crompton M, Dubinsky JM. Increased susceptibility of striatal mitochondria to calcium-induced permeability transition. J Neurosci. 2003; 23:4858–4867. [PubMed: 12832508]

Buckman JF, Hernandez H, Kress GJ, Votyakova TV, Pal S, Reynolds IJ. MitoTracker labeling in primary neuronal and astrocytic cultures: influence of mitochondrial membrane potential and oxidants. J Neurosci Methods. 2001; 104:165–176. [PubMed: 11164242]

Chang DT, Reynolds IJ. Mitochondrial trafficking and morphology in healthy and injured neurons. Prog Neurobiol. 2006; 80:241–268. [PubMed: 17188795]

Chesselet MF. In vivo alpha-synuclein overexpression in rodents: a useful model of Parkinson's disease? Exp Neurol. 2008; 209:22–27. [PubMed: 17949715]

Conway KA, Harper JD, Lansbury PT. Accelerated in vitro fibril formation by a mutant alpha-synuclein linked to early-onset Parkinson disease. Nat Med. 1998; 4:1318–1320. [PubMed: 9809558]

Conway KA, Lee SJ, Rochet JC, Ding TT, Williamson RE, Lansbury PT Jr. Acceleration of oligomerization, not fibrillization, is a shared property of both alpha-synuclein mutations linked to early-onset Parkinson's disease: implications for pathogenesis and therapy. Proc Natl Acad Sci U S A. 2000; 97:571–576. [PubMed: 10639120]

Cookson MR, van der Brug M. Cell systems and the toxic mechanism(s) of alpha-synuclein. Exp Neurol. 2008; 209:5–11. [PubMed: 17603039]

Cortassa S, Aon MA, Marban E, Winslow RL, O'Rourke B. An integrated model of cardiac mitochondrial energy metabolism and calcium dynamics. Biophys J. 2003; 84:2734–2755. [PubMed: 12668482]

Crews L, Mizuno H, Desplats P, Rockenstein E, Adame A, Patrick C, Winner B, Winkler J, Masliah E. Alpha-synuclein alters Notch-1 expression and neurogenesis in mouse embryonic stem cells and in the hippocampus of transgenic mice. J Neurosci. 2008; 28:4250–4260. [PubMed: 18417705]

Crompton M. The mitochondrial permeability transition pore and its role in cell death. Biochem J. 1999; 341 (Pt 2):233–249. [PubMed: 10393078]

Cuervo AM. Autophagy: in sickness and in health. Trends Cell Biol. 2004; 14:70–77. [PubMed: 15102438]

Cuervo AM, Bergamini E, Brunk UT, Droge W, Ffrench M, Terman A. Autophagy and aging: the importance of maintaining "clean" cells. Autophagy. 2005; 1:131–140. [PubMed: 16874025]

Cuervo AM, Stefanis L, Fredenburg R, Lansbury PT, Sulzer D. Impaired degradation of mutant alpha-synuclein by chaperone-mediated autophagy. Science. 2004; 305:1292–1295. [PubMed: 15333840]

Danzer KM, Haasen D, Karow AR, Moussaud S, Habeck M, Giese A, Kretzschmar H, Hengerer B, Kostka M. Different species of alpha-synuclein oligomers induce calcium influx and seeding. J Neurosci. 2007; 27:9220–9232. [PubMed: 17715357]

Dauer W, Kholodilov N, Vila M, et al. Resistance of alpha -synuclein null mice to the parkinsonian neurotoxin MPTP. Proc Natl Acad Sci U S A. 2002; 99:14524–14529. [PubMed: 12376616]

Dauer W, Przedborski S. Parkinson's disease: mechanisms and models. Neuron. 2003; 39:889–909. [PubMed: 12971891]

Deng H, Dodson MW, Huang H, Guo M. The Parkinson's disease genes pink1 and parkin promote mitochondrial fission and/or inhibit fusion in Drosophila. Proc Natl Acad Sci U S A. 2008; 105:14503–14508. [PubMed: 18799731]

Deng H, Jankovic J, Guo Y, Xie W, Le W. Small interfering RNA targeting the PINK1 induces apoptosis in dopaminergic cells SH-SY5Y. Biochem Biophys Res Commun. 2005; 337:1133–1138. [PubMed: 16226715]

Devi L, Raghavendran V, Prabhu BM, Avadhani NG, Anandatheerthavarada HK. Mitochondrial import and accumulation of alpha-synuclein impair complex I in human dopaminergic neuronal cultures and Parkinson disease brain. J Biol Chem. 2008; 283:9089–9100. [PubMed: 18245082]

Dunn WA Jr. Autophagy and related mechanisms of lysosome-mediated protein degradation. Trends Cell Biol. 1994; 4:139–143. [PubMed: 14731737]

Elkon H, Don J, Melamed E, Ziv I, Shirvan A, Offen D. Mutant and wild-type alpha-synuclein interact with mitochondrial cytochrome C oxidase. J Mol Neurosci. 2002; 18:229–238. [PubMed: 12059041]

Exner N, Treske B, Paquet D, et al. Loss-of-function of human PINK1 results in mitochondrial pathology and can be rescued by parkin. J Neurosci. 2007; 27:12413–12418. [PubMed: 17989306]

Furukawa K, Matsuzaki-Kobayashi M, Hasegawa T, et al. Plasma membrane ion permeability induced by mutant alpha-synuclein contributes to the degeneration of neural cells. J Neurochem. 2006; 97:1071–1077. [PubMed: 16606366]

Giasson BI, Duda JE, Quinn SM, Zhang B, Trojanowski JQ, Lee VM. Neuronal alpha-Synucleinopathy with Severe Movement Disorder in Mice Expressing A53T Human alpha-Synuclein. Neuron. 2002; 34:521–533. [PubMed: 12062037]

Green DR, Reed JC. Mitochondria and apoptosis. Science. 1998; 281:1309–1312. [PubMed: 9721092]

Haque ME, Thomas KJ, D'Souza C, et al. Cytoplasmic Pink1 activity protects neurons from dopaminergic neurotoxin MPTP. Proc Natl Acad Sci U S A. 2008; 105:1716–1721. [PubMed: 18218782]

Hasegawa M, Fujiwara H, Nonaka T, Wakabayashi K, Takahashi H, Lee VM, Trojanowski JQ, Mann D, Iwatsubo T. Phosphorylated alpha-synuclein is ubiquitinated in alpha-synucleinopathy lesions. J Biol Chem. 2002; 277:49071–49076. [PubMed: 12377775]

Hashimoto M, Takenouchi T, Rockenstein E, Masliah E. Alpha-synuclein up-regulates expression of caveolin-1 and down-regulates extracellular signal-regulated kinase activity in B103 neuroblastoma cells: role in the pathogenesis of Parkinson's disease. J Neurochem. 2003; 85:1468–1479. [PubMed: 12787066]

Hashimoto M, Yoshimoto M, Sisk A, Hsu LJ, Sundsmo M, Kittel A, Saitoh T, Miller A, Masliah E. NACP, a synaptic protein involved in Alzheimer's disease, is differentially regulated during megakaryocyte differentiation. Biochem Biophys Res Commun. 1997; 237:611–616. [PubMed: 9299413]

Hatano Y, Li Y, Sato K, et al. Novel PINK1 mutations in early-onset parkinsonism. Ann Neurol. 2004; 56:424–427. [PubMed: 15349870]

Hedrich K, Hagenah J, Djarmati A, et al. Clinical spectrum of homozygous and heterozygous PINK1 mutations in a large German family with Parkinson disease: role of a single hit? Arch Neurol. 2006; 63:833–838. [PubMed: 16769864]

Heikkila RE, Nicklas WJ, Vyas I, Duvoisin RC. Dopaminergic toxicity of rotenone and the 1-methyl-4-phenylpyridinium ion after their stereotaxic administration to rats: implication for the mechanism of 1-methyl-4-phenyl-1,2,3,6-tetrahydropyridine toxicity. Neurosci Lett. 1985; 62:389–394. [PubMed: 3912685]

Hirsch EC, Hunot S, Faucheux B, Agid Y, Mizuno Y, Mochizuki H, Tatton WG, Tatton N, Olanow WC. Dopaminergic neurons degenerate by apoptosis in Parkinson's disease. Mov Disord. 1999; 14:383–385. [PubMed: 10091646]

Hsu LJ, Sagara Y, Arroyo A, et al. alpha-synuclein promotes mitochondrial deficit and oxidative stress. Am J Pathol. 2000; 157:401–410. [PubMed: 10934145]

Langford D, Grigorian A, Hurford R, Adame A, Crews L, Masliah E. The role of mitochondrial alterations in the combined toxic effects of human immunodeficiency virus Tat protein and methamphetamine on calbindin positive-neurons. J Neurovirol. 2004; 10:327–337. [PubMed: 15765804]

Langston JW, Ballard P, Tetrud JW, Irwin I. Chronic Parkinsonism in humans due to a product of meperidine-analog synthesis. Science. 1983; 219:979–980. [PubMed: 6823561]

Lee M, Hyun D, Halliwell B, Jenner P. Effect of the overexpression of wild-type or mutant alpha-synuclein on cell susceptibility to insult. J Neurochem. 2001; 76:998–1009. [PubMed: 11181819]

Lee MK, Stirling W, Xu Y, et al. Human alpha-synuclein-harboring familial Parkinson's disease-linked Ala-53 --> Thr mutation causes neurodegenerative disease with alpha-synuclein aggregation in transgenic mice. Proc Natl Acad Sci U S A. 2002; 99:8968–8973. [PubMed: 12084935]

Leng Y, Chase TN, Bennett MC. Muscarinic receptor stimulation induces translocation of an alpha-synuclein oligomer from plasma membrane to a light vesicle fraction in cytoplasm. J Biol Chem. 2001; 276:28212–28218. [PubMed: 11337491]

Li WW, Yang R, Guo JC, Ren HM, Zha XL, Cheng JS, Cai DF. Localization of alpha-synuclein to mitochondria within midbrain of mice. Neuroreport. 2007; 18:1543–1546. [PubMed: 17885598]

Liu S, Ninan I, Antonova I, et al. alpha-Synuclein produces a long-lasting increase in neurotransmitter release. Embo J. 2004; 23:4506–4516. [PubMed: 15510220]

Martin LJ, Pan Y, Price AC, Sterling W, Copeland NG, Jenkins NA, Price DL, Lee MK. Parkinson's disease alpha-synuclein transgenic mice develop neuronal mitochondrial degeneration and cell death. J Neurosci. 2006; 26:41–50. [PubMed: 16399671]

Martinez J, Moeller I, Erdjument-Bromage H, Tempst P, Lauring B. Parkinson's disease-associated alpha-synuclein is a calmodulin substrate. J Biol Chem. 2003; 278:17379–17387. [PubMed: 12610000]

Masliah E, Rockenstein E, Veinbergs I, Mallory M, Hashimoto M, Takeda A, Sagara, Sisk A, Mucke L. Dopaminergic loss and inclusion body formation in alpha-synuclein mice: Implications for neurodegenerative disorders. Science. 2000; 287:1265–1269. [PubMed: 10678833]

Masliah E, Sisk A, Mallory M, Games D. Neurofibrillary pathology in transgenic mice overexpressing V717F beta-amyloid precursor protein. J Neuropathol Exp Neurol. 2001; 60:357–368. [PubMed: 11305871]

Mattson MP. Calcium and neurodegeneration. Aging Cell. 2007; 6:337–350. [PubMed: 17328689]

McCormack JG, Halestrap AP, Denton RM. Role of calcium ions in regulation of mammalian intramitochondrial metabolism. Physiol Rev. 1990; 70:391–425. [PubMed: 2157230]

Mizuno Y, Ohta S, Tanaka M, Takamiya S, Suzuki K, Sato T, Oya H, Ozawa T, Kagawa Y. Deficiencies in complex I subunits of the respiratory chain in Parkinson's disease. Biochem Biophys Res Commun. 1989; 163:1450–1455. [PubMed: 2551290]

Nakada K, Inoue K, Ono T, Isobe K, Ogura A, Goto YI, Nonaka I, Hayashi JI. Inter-mitochondrial complementation: Mitochondria-specific system preventing mice from expression of disease phenotypes by mutant mtDNA. Nat Med. 2001; 7:934–940. [PubMed: 11479626]

Naldini L, Verma IM. Lentiviral vectors. Adv Virus Res. 2000; 55:599–609. [PubMed: 11050959]

Narhi L, Wood SJ, Steavenson S, et al. Both familial Parkinson's disease mutations accelerate alpha-synuclein aggregation. J Biol Chem. 1999; 274:9843–9846. [PubMed: 10092675]

Nicholls DG, Budd SL. Mitochondria and neuronal survival. Physiol Rev. 2000; 80:315–360. [PubMed: 10617771]

Nicholls DG, Crompton M. Mitochondrial calcium transport. FEBS Lett. 1980; 111:261–268. [PubMed: 6987089]

Ono T, Isobe K, Nakada K, Hayashi JI. Human cells are protected from mitochondrial dysfunction by complementation of DNA products in fused mitochondria. Nat Genet. 2001; 28:272–275. [PubMed: 11431699]

Orth M, Schapira AH. Mitochondria and degenerative disorders. Am J Med Genet. 2001; 106:27–36. [PubMed: 11579422]

Pallanck L, Greenamyre JT. Neurodegenerative disease: pink, parkin and the brain. Nature. 2006; 441:1058. [PubMed: 16810237]

Pan T, Kondo S, Le W, Jankovic J. The role of autophagy-lysosome pathway in neurodegeneration associated with Parkinson's disease. Brain. 2008

Panov AV, Gutekunst CA, Leavitt BR, Hayden MR, Burke JR, Strittmatter WJ, Greenamyre JT. Early mitochondrial calcium defects in Huntington's disease are a direct effect of polyglutamines. Nat Neurosci. 2002; 5:731–736. [PubMed: 12089530]

Parihar MS, Parihar A, Fujita M, Hashimoto M, Ghafourifar P. Mitochondrial association of alpha-synuclein causes oxidative stress. Cell Mol Life Sci. 2008; 65:1272–1284. [PubMed: 18322646]

Petit A, Kawarai T, Paitel E, et al. Wild-type PINK1 prevents basal and induced neuronal apoptosis, a protective effect abrogated by Parkinson disease-related mutations. J Biol Chem. 2005; 280:34025–34032. [PubMed: 16079129]

Pickford F, Masliah E, Britschgi M, et al. The autophagy-related protein beclin 1 shows reduced expression in early Alzheimer disease and regulates amyloid beta accumulation in mice. J Clin Invest. 2008; 118:2190–2199. [PubMed: 18497889]

Priault M, Salin B, Schaeffer J, Vallette FM, di Rago JP, Martinou JC. Impairing the bioenergetic status and the biogenesis of mitochondria triggers mitophagy in yeast. Cell Death Differ. 2005; 12:1613–1621. [PubMed: 15947785]

Pridgeon JW, Olzmann JA, Chin LS, Li L. PINK1 Protects against Oxidative Stress by Phosphorylating Mitochondrial Chaperone TRAP1. PLoS Biol. 2007; 5:e172. [PubMed: 17579517]

Ravikumar B, Duden R, Rubinsztein DC. Aggregate-prone proteins with polyglutamine and polyalanine expansions are degraded by autophagy. Hum Mol Genet. 2002; 11:1107–1117. [PubMed: 11978769]

Rintoul GL, Bennett VJ, Papaconstandinou NA, Reynolds IJ. Nitric oxide inhibits mitochondrial movement in forebrain neurons associated with disruption of mitochondrial membrane potential. J Neurochem. 2006; 97:800–806. [PubMed: 16573650]

Rockenstein E, Mallory M, Mante M, Sisk A, Masliah E. Early formation of mature amyloid-b proteins deposits in a mutant APP transgenic model depends on levels of Ab1–42. J neurosci Res. 2001; 66:573–582. [PubMed: 11746377]

Rubinsztein DC. The roles of intracellular protein-degradation pathways in neurodegeneration. Nature. 2006; 443:780–786. [PubMed: 17051204]

Schapira AH, Cooper JM, Dexter D, Jenner P, Clark JB, Marsden CD. Mitochondrial complex I deficiency in Parkinson's disease. Lancet. 1989; 1:1269. [PubMed: 2566813]

Schubert D, Heinemann S, Carlisle W, Tarikas H, Kimes B, Patrick J, Steinbach JH, Culp W, Brandt BL. Clonal cell lines from the rat central nervous system. Nature. 1974; 249:224–227. [PubMed: 4151463]

Seglen PO, Bohley P. Autophagy and other vacuolar protein degradation mechanisms. Experientia. 1992; 48:158–172. [PubMed: 1740188]

Silvestri L, Caputo V, Bellacchio E, Atorino L, Dallapiccola B, Valente EM, Casari G. Mitochondrial import and enzymatic activity of PINK1 mutants associated to recessive parkinsonism. Hum Mol Genet. 2005; 14:3477–3492. [PubMed: 16207731]

Smith WW, Jiang H, Pei Z, Tanaka Y, Morita H, Sawa A, Dawson VL, Dawson TM, Ross CA. Endoplasmic reticulum stress and mitochondrial cell death pathways mediate A53T mutant alpha-synuclein-induced toxicity. Hum Mol Genet. 2005; 14:3801–3811. [PubMed: 16239241]

Souza J, Giasson B, Lee VY, Ischiropoulos H. Chaperone-like activity of synucleins. FEBS Lett. 2000; 474:116–119. [PubMed: 10828462]

Spillantini M, Schmidt M, Lee VY, Trojanowski J, Jakes R, Goedert M. α-Synuclein in Lewy bodies. Nature. 1997; 388:839–840. [PubMed: 9278044]

Takeda A, Mallory M, Sundsmo M, Honer W, Hansen L, Masliah E. Abnormal accumulation of NACP/α-synuclein in neurodegenerative disorders. Am J Pathol. 1998; 152:367–372. [PubMed: 9466562]

Takenouchi T, Hashimoto M, Hsu L, Mackowski B, Rockenstein E, Mallory M, Masliah E. Reduced neuritic outgrowth and cell adhesion in neuronal cells transfected with human α-synuclein. Mol Cell Neurosci. 2001; 17:141–150. [PubMed: 11161475]

Tan EK, Skipper LM. Pathogenic mutations in Parkinson disease. Hum Mutat. 2007; 28:641–653. [PubMed: 17385668]

Thyagarajan D, Bressman S, Bruno C, Przedborski S, Shanske S, Lynch T, Fahn S, DiMauro S. A novel mitochondrial 12SrRNA point mutation in parkinsonism, deafness, and neuropathy. Ann Neurol. 2000; 48:730–736. [PubMed: 11079536]

Valente EM, Abou-Sleiman PM, Caputo V, et al. Hereditary early-onset Parkinson's disease caused by mutations in PINK1. Science. 2004; 304:1158–1160. [PubMed: 15087508]

Ventruti A, Cuervo AM. Autophagy and neurodegeneration. Curr Neurol Neurosci Rep. 2007; 7:443–451. [PubMed: 17764636]

Volles MJ, Lansbury PT Jr. Vesicle permeabilization by protofibrillar alpha-synuclein is sensitive to Parkinson's disease-linked mutations and occurs by a pore-like mechanism. Biochemistry. 2002; 41:4595–4602. [PubMed: 11926821]

Wakabayashi K, Matsumoto K, Takayama K, Yoshimoto M, Takahashi H. NACP, a presynaptic protein, immunoreactivity in Lewy bodies in Parkinson's disease. Neurosci Lett. 1997; 239:45–48. [PubMed: 9547168]

Waldmeier PC, Zimmermann K, Qian T, Tintelnot-Blomley M, Lemasters JJ. Cyclophilin D as a drug target. Curr Med Chem. 2003; 10:1485–1506. [PubMed: 12871122]

Webb JL, Ravikumar B, Atkins J, Skepper JN, Rubinsztein DC. Alpha-Synuclein is degraded by both autophagy and the proteasome. J Biol Chem. 2003; 278:25009–25013. [PubMed: 12719433]

Yang Y, Ouyang Y, Yang L, Beal MF, McQuibban A, Vogel H, Lu B. Pink1 regulates mitochondrial dynamics through interaction with the fission/fusion machinery. Proc Natl Acad Sci U S A. 2008; 105:7070–7075. [PubMed: 18443288]

Yu S, Zuo X, Li Y, Zhang C, Zhou M, Zhang YA, Ueda K, Chan P. Inhibition of tyrosine hydroxylase expression in alpha-synuclein-transfected dopaminergic neuronal cells. Neurosci Lett. 2004; 367:34–39. [PubMed: 15308292]

Zanelli SA, Trimmer PA, Solenski NJ. Nitric oxide impairs mitochondrial movement in cortical neurons during hypoxia. J Neurochem. 2006; 97:724–736. [PubMed: 16606371]

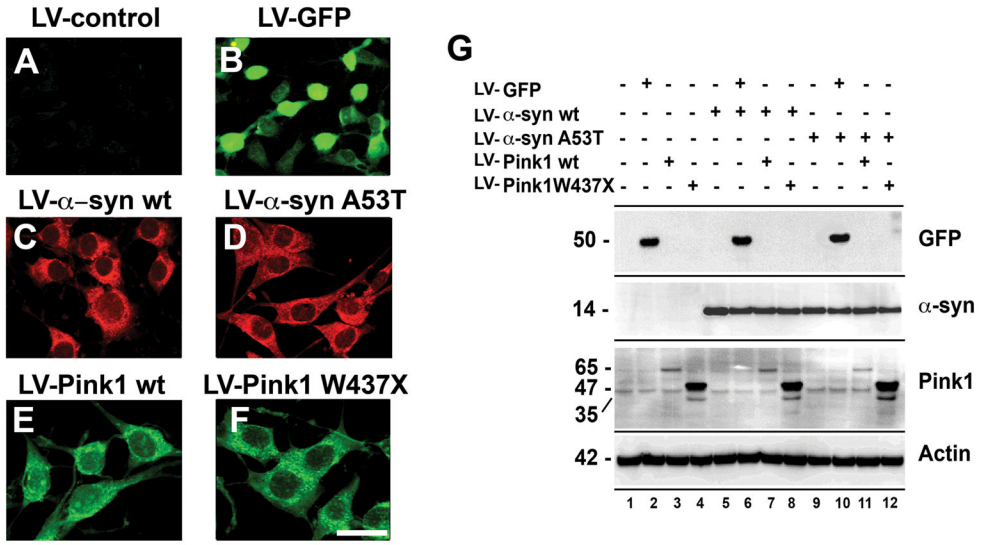

Fig. 1.

Characterization of levels of expression in B103 neuronal cells infected with LV α-syn and Pink1. (A) In samples infected with empty vector no fluorescent signal was detected. (B) Abundant signal was detected in cells infected with LV-GFP. (C and D) Detection by immunoflourescence microscopy of α-syn expression in cells infected with LV-α-syn wt or LV-α-syn A53T. (E and F) Immunoflourescence detection of Pink1 with an antibody against HA in cells infected with LV-Pink1 wt or LV-Pink1 W437X. (G) Western blot analysis of homogenates from neuronal cells infected with LV-GFP, LV-α-syn or LV-Pink1. Scale bar (20μm) in panel (F) applies to all photographs.

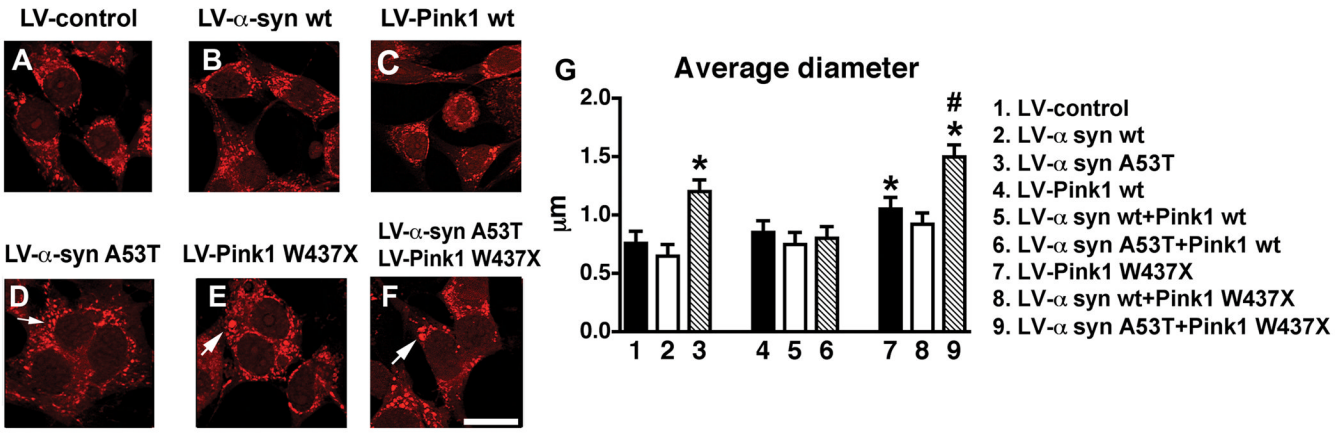

Fig. 2.

Analysis of mitochondrial morphology by Mitotracker in neuronal cells infected with LV expressing α-syn and Pink1. (A-C) Baseline appearance of mitochondria (arrows) in neuronal cells infected with LV-empty control, α-syn wt and Pink1 wt. (D-F) Enlarged mitochondria (arrows) in neuronal cells infected with LV-α-syn A53T and/or Pink1 W437X. (G) Image analysis of mean mitochondrial diameter. An average of 200 cells per condition were recorded by laser confocal microscopy and analyzed with the NIH Image J program. Cells expressing α-syn A53T or Pink1 W437X showed a 25–50% increase in mitochondrial size. These alterations were exacerbated in cells co-infected with LV-α-syn A53T and LV-Pink1 W437X. *$p < 0.05$ compared to cells infected with LV-control by one-way ANOVA followed by post-hoc Dunnett's test; #$p < 0.05$ compared to cells singly-infected with LV-α-syn A53T or LV-Pink1 W437X by one-way ANOVA followed by post-hoc Tukey-Kramer test. Scale bar (5μm) in panel (F) applies to all photographs.

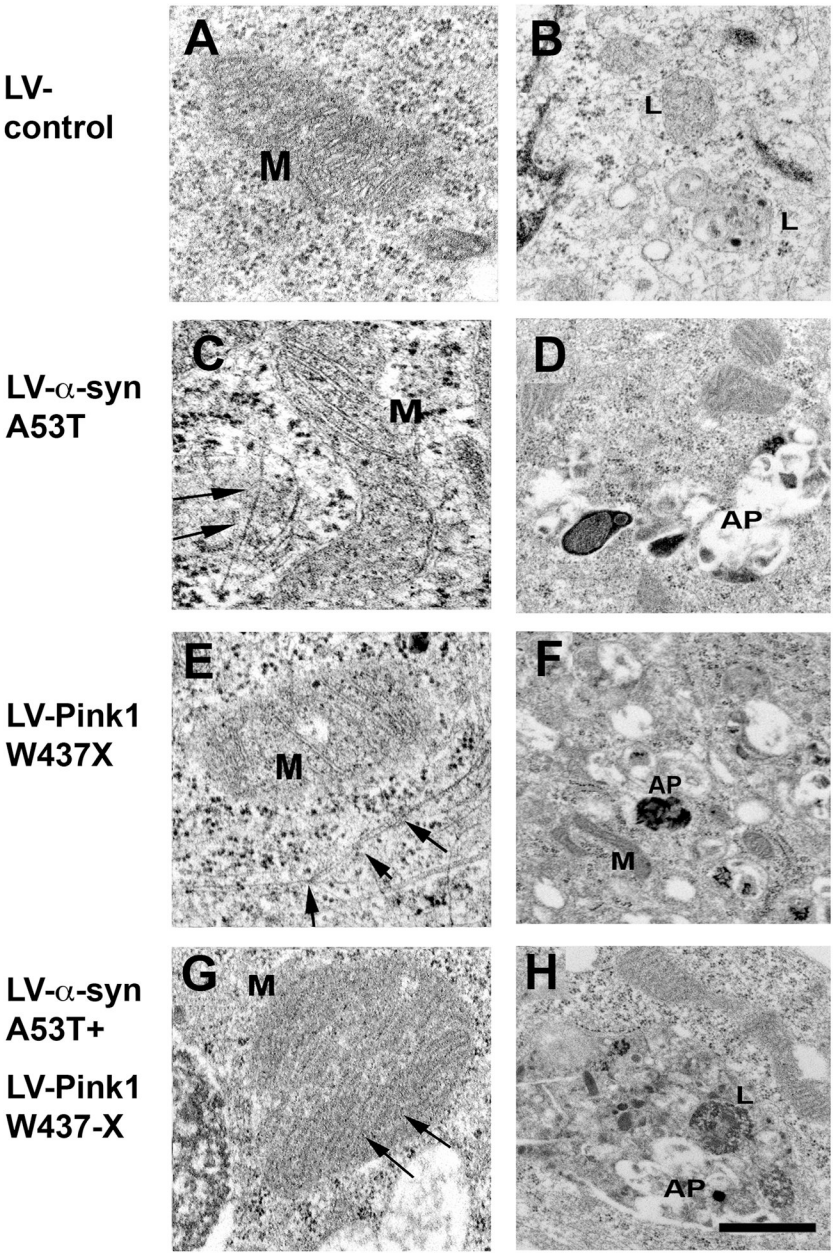

Fig. 3.

Ultrastructural analysis of neuronal cells infected with LV expressing α-syn and Pink1. (A and B) Cells infected with LV-control display preservation of the baseline structure of mitochondria (M), rough endoplasmic reticulum, and lysosomes (L). (D-F) In neuronal cells infected with either LV-α-syn A53T (C and D) or Pink1 W437X (E and F) the mitochondria (M) were elongated and often surrounded by filaments (arrows). In addition, in the cytoplasm there were abundant electrodense laminar structures reminiscent of autophagolysosomes (AP). (G and H) Neuronal cells co-infected with LV-α-syn A53T and Pink1 W437X displayed the presence of enlarged mitochondria with redundant cristae (arrows) and abnormal lysosomes (L) with electrodense material and autophagolysosomes (AP). Scale bar (0.5μm) in panel (G) applies to panels A, C, E, G; scale bar (1μm) in panel (H) applies to panels B, D, F, H.

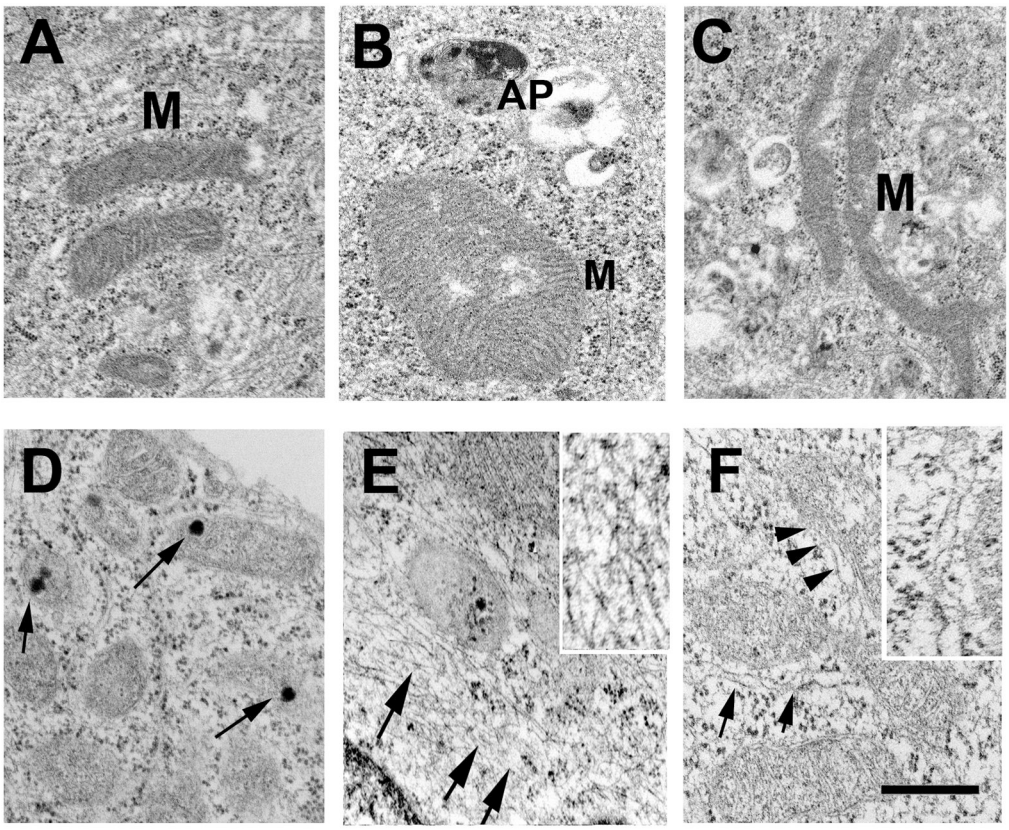

Fig. 4.

Characterization of the mitochondrial pathology in a neuronal cell line infected with LV expressing mutant α-syn and Pink1. (A) Preserved mitochondria (M) morphology in cells infected with the LV-control. (B, C) Enlarged and elongated mitochondria were found in the proximity of autophagolysosomes (AP) in cells co-infected with LV-α-syn A53T and Pink1 W437X. (D) Accumulation of abnormal electrodense granules (arrows) in the mitochondrial matrix in cells co-infected with LV-α-syn A53T and Pink1 W437X. (E, F) Abnormal mitochondria surrounded by filaments (arrowheads) and autophagolysosomes in cells co-infected with LV-α-syn A53T and Pink1 W437X. Insets show higher-power image of peri-mitochondrial filaments. Scale bar (0.25μm) in panel (F) applies to all micrographs.

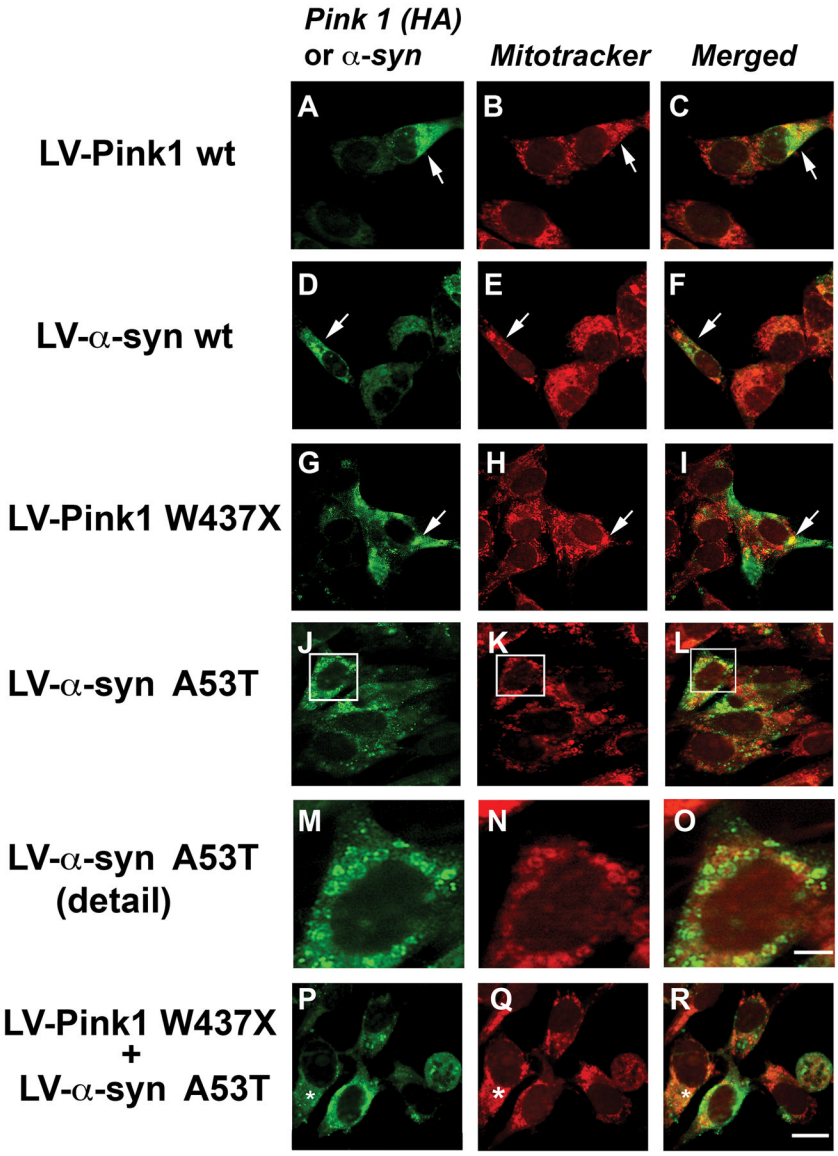

Fig. 5.

Co-localization of α-syn and Pink1 with mitochondria in neuronal cells infected with LV. Cells were grown on coverslips, labeled with Mitotracker Red, immunostained with antibodies against α-syn or HA to detect Pink1 and imaged with the laser confocal microscope. (A-C) Cells expressing Pink1 wt or (D-F) α-syn wt displayed a more diffuse immunoreactivity (arrows). (G-I) In cells infected with LV-Pink1 W437X or (J-L) LV-α-syn A53T the immunoreactivity for Pink1 or α-syn was in closer proximity to mitochondria stained with Mitotracker (arrows). (M-O) Close-up of the image indicated by the box. (P-R) Co-localization of mutant α-syn and Mitotracker became more evident in cells co-infected with LV-α-syn A53T and LV-Pink1 W437X (*). Scale bar (5μm) in panel (R) applies to panels A-L and P-R; scale bar (2μm) in panel (O) applies to panels M-O.

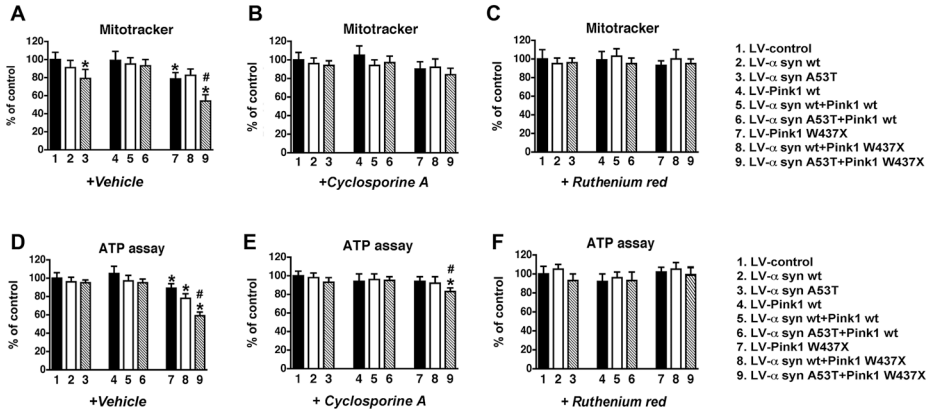

Fig. 6.

Functional mitochondrial alterations, and the protective effects of cyclosporine A and Ruthenium red, in B103 cells infected with LV expressing α-syn and Pink1. All values are expressed as percent of control. Neuronal cells were treated with 5μM cyclosporine A or 10mM Ruthenium red. (A-C) Semi-quantitative analysis of the mitochondrial $\Delta\Psi_m$ by Mitotracker Red fluorescence in cells treated with vehicle control (A), cyclosporine A (B), or Ruthenium red (C). (D-F) Determination (by luminescent assay kit) of ATP production in cells treated with vehicle control (D), cyclosporine A (E) and Ruthenium red (F). Cells expressing mutant α-syn and Pink1 showed a reduction in mitochondrial function and ATP production, this effect being greater in cells expressing both mutant proteins. Treatment with cyclosporine A partially reduced the deficits in cells expressing mutant α-syn and Pink1, while Ruthenium red fully reverted the effects of the combined mutant proteins. *$p < 0.05$ compared to LV-control by one-way ANOVA followed by post-hoc Dunnett's test; #$p < 0.05$ compared to cells singly-infected with LV-α-syn A53T or LV-Pink1 W437X by one-way ANOVA followed by post-hoc Tukey-Kramer test.

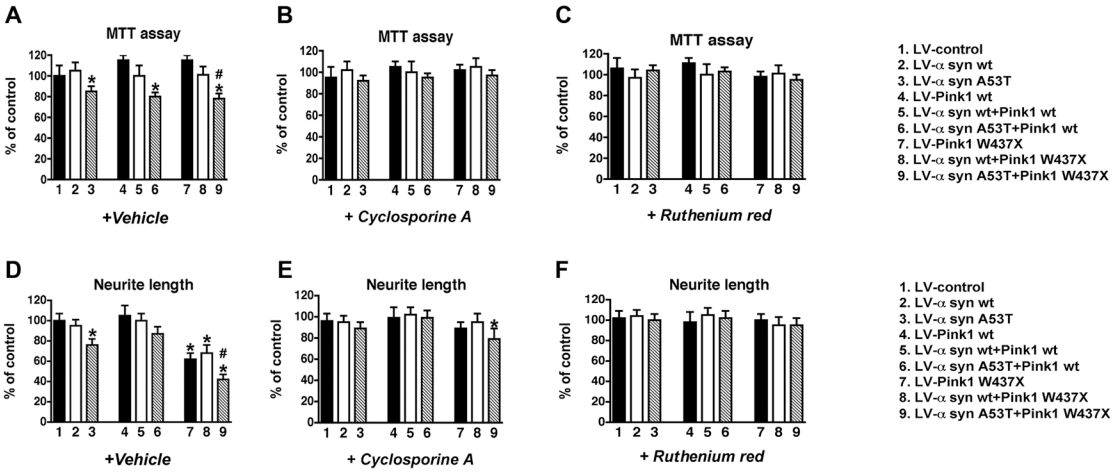

Fig. 7.

Neuronal alterations and the protective effects of cyclosporine A and Ruthenium red, in B103 cells infected with LV expressing α-syn and Pink1. All values are expressed as percent of control. Neuronal cells were treated with 5μM cyclosporine A or 10μM Ruthenium red. (A-C) MTT assay in cells treated with vehicle control (A), Cyclosporine A (B), or Ruthenium red (C). (D-F) Determination of neurite length by phase contrast microscopy and image analysis of cells treated with vehicle control (D), Cyclosporine A (E), or Ruthenium red (F). Cells expressing mutant α-syn and Pink1 showed a reduction in mitochondrial activity and neurite lengths, this effect being greater in cells expressing both mutant proteins. Treatment with cyclosporine A partially reduced the deficits in cells expressing mutant α-syn and Pink1, while Ruthenium red fully reverted the effects of the combined mutant proteins. *$p < 0.05$ compared to LV-control by one-way ANOVA followed by post-hoc Dunnett's test; #$p < 0.05$ compared to cells singly-infected with LV-α-syn A53T or LV-Pink1 W437X by one-way ANOVA followed by post-hoc Tukey-Kramer test.

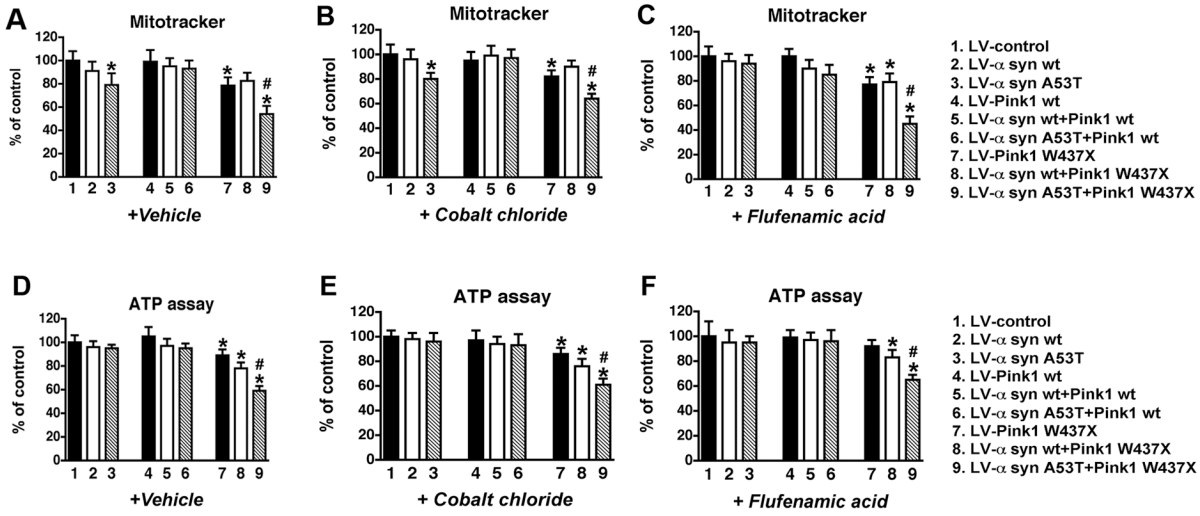

Fig. 8.

Effects of calcium blockers on membrane potential and ATP production in a neuronal cell line infected with LV expressing α-syn and Pink1. All values are expressed as percent of control. Neuronal cells were treated with cellular calcium inhibitors cobalt chloride (5μM), or flufenamic acid (40μM) and analyzed with Mitotracker Red or by ATP assay. (A-C) Semi-quantitative analysis of the mitochondrial $\Delta\Psi_m$ by Mitotracker Red fluorescence in cells treated with vehicle control (A), Cobalt chloride (B), or Flufenamic acid (C). (D-F) Determination (by luminescent assay kit) of ATP production in cells treated with vehicle control (D), Cobalt chloride (E), or Flufenamic acid (F). In contrast to the protective effects of Ruthenium red, neither of the other calcium blockers reverted the effects of expressing mutant α-syn and Pink1 on the $\Delta\Psi_m$ or ATP production. *$p < 0.05$ compared to LV-control by one-way ANOVA followed by post-hoc Dunnett's test; #$p < 0.05$ compared to cells singly-infected with LV-α-syn A53T or LV-Pink1 W437X by one-way ANOVA followed by post-hoc Tukey-Kramer test.

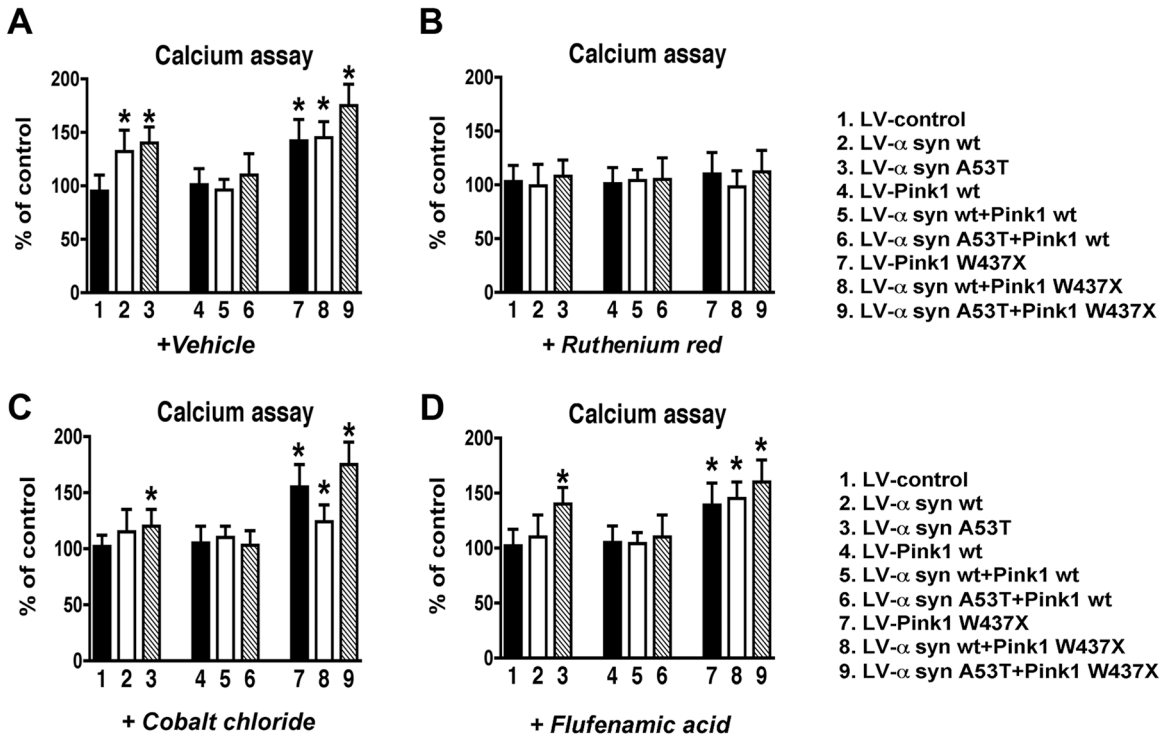

Fig. 9.

Effects of calcium blockers on intracellular calcium levels in neuronal cells expressing α-syn and Pink1. All values are expressed as percent of control. Neuronal cells were incubated with cellular calcium inhibitors ruthenium red (10μM), cobalt chloride (5μM), or flufenamic acid (40μM) followed by treatment with calcium dye and analyzed by fluorescence microscopy on a spectrophotomer. (A) Calcium levels in cells treated with vehicle control. (B) Calcium levels in cells treated with Ruthenium red. (C) Calcium levels in cells treated with Cobalt chloride. (D) Calcium levels in cells treated with Flufenamic acid. As for $\Delta\Psi_m$, treatment with ruthenium red was able to revert the effects of co-expressed mutant proteins on calcium influx. *$p < 0.05$ compared to LV-control by one-way ANOVA followed by post-hoc Dunnett's test.